Amplification of Galactic Magnetic Fields by the Cosmic-Ray Driven Dynamo

M. Hanasz[1]

G. Kowal[2], K. Otmianowska-Mazur[2]
and

H. Lesch[3]

ABSTRACT

We present the first numerical model of the magnetohydrodynamical cosmic-ray (CR) driven dynamo of the type proposed by Parker (1992). The driving force of the amplification process comes from CRs injected into the galactic disk in randomly distributed spherical regions representing supernova remnants. The underlying disk is differentially rotating. An explicit resistivity is responsible for the dissipation of the small-scale magnetic field component. We obtain amplification of the large-scale magnetic on a timescale 250 Myr.

Subject headings: Galaxies: ISM, Magnetic Fields; ISM: Cosmic Rays, Magnetic Fields; MHD: Dynamos

1. Introduction

In 1992 Parker discussed the possibility of a new kind of galactic dynamo driven by galactic CRs accelerated in supernova remnants. This dynamo contains a network of interacting forces: the buoyancy force of CRs, the Coriolis force, the differential rotation and magnetic reconnection. Parker estimated that such a dynamo is able to amplify the large scale magnetic field on timescales of the order of 10^8yr.

Over the last decade we have investigated the different physical properties and consequences of Parker's idea and scenario by means of analytical calculations and numerical simulations (see eg. Hanasz & Lesch 1998, Lesch & Hanasz 2003 and references therein). Here we present the first complete magnetohydrodynamical three-dimensional simulation including the full network of relevant interacting mechanisms.

It is the aim of our contribution to show that Parker's CR driven dynamo indeed acts efficiently on timescales comparable with the disk rotation time. In the next two Sections we describe the physical elements of the model and the system of equations used in numerical simulations. Section 4 presents the numerical setup, Sections 5 and 6 inform the reader about the results on the structure of the interstellar medium including CRs and magnetic fields, the strength of the amplified magnetic field and the spatial structure of the mean magnetic field. We summarize our results very briefly in Section 7.

2. Elements of the model

We performed computations with the aid of the Zeus-3D MHD code (Stone & Norman 1992a,b), which we extended with the following features:

(1) The CR component, a relativistic gas de-

[1]Centre for Astronomy, Nicholas Copernicus University, PL-87148 Piwnice/Toruń, Poland, mhanasz@astri.uni.torun.pl

[2]Astronomical Observatory, Jagiellonian University, ul. Orla 171, 30-244 Kraków, kowal@oa.uj.edu.pl, otmian@oa.uj.edu.pl

[3]Astronomical Observatory, Munich University, Scheinerstr. 1, D-81679, Germany, lesch@usm.uni-muenchen.de

scribed by the diffusion-advection transport equation (see Hanasz & Lesch 2003b for the details of numerical algorithm). Following Jokipii (1999) we presume that CRs diffuse anisotropically along magnetic field lines. (2) Localized sources of CRs: supernova remnants, exploding randomly in the disk volume (see Hanasz & Lesch 2000). (3) Resistivity of the ISM (see Hanasz et al. 2002, Hanasz & Lesch 2003a) responsible for the onset of fast magnetic reconnection (in this paper we apply the uniform resistivity). (4) Shearing boundary conditions and tidal forces, following the prescription by Hawley, Gammie & Balbus (1995), aimed to model differentially rotating disks in the local approximation. (5) Realistic vertical disk gravity following the model of ISM in the Milky Way by Ferriere (1998).

3. The system of equations

We apply the following set of resistive MHD equations

$$\frac{\partial \rho}{\partial t} + \boldsymbol{\nabla} \cdot (\rho \boldsymbol{V}) = 0, \tag{1}$$

$$\frac{\partial e}{\partial t} + \boldsymbol{\nabla} \cdot (e \boldsymbol{V}) = -p \left(\boldsymbol{\nabla} \cdot \boldsymbol{V} \right), \tag{2}$$

$$\frac{\partial \boldsymbol{V}}{\partial t} + (\boldsymbol{V} \cdot \boldsymbol{\nabla}) \boldsymbol{V} = -\frac{1}{\rho} \boldsymbol{\nabla} \left(p + p_{\rm cr} + \frac{B^2}{8\pi} \right) + \frac{\boldsymbol{B} \cdot \boldsymbol{\nabla} \boldsymbol{B}}{4\pi\rho} - 2\boldsymbol{\Omega} \times \boldsymbol{v} + 2q\Omega^2 {\rm x} \hat{\boldsymbol{e}}_{\rm x} + {\rm g_z} \hat{\boldsymbol{e}}_{\rm z}, \tag{3}$$

$$\frac{\partial \boldsymbol{B}}{\partial t} = \boldsymbol{\nabla} \times (\boldsymbol{V} \times \boldsymbol{B}) + \eta \Delta \boldsymbol{B}, \tag{4}$$

$$p = (\gamma - 1) e, \quad \gamma = 5/3 \tag{5}$$

where q $= -$d lnΩ/d lnR is the shearing parameter, (R is the distance to galactic center), g_z is the vertical gravitational acceleration, η is the resistivity, γ is the adiabatic index of thermal gas, the gradient of CR pressure ∇p_{cr} is included in the equation of motion (see Hanasz & Lesch 2003b) and other symbols have their usual meaning. The uniform resistivity is included only in the induction equation (see Hanasz et al. 2002). The adopted value $\eta = 1$ exceeds the numerical resistivity for the grid resolution defined in the next section (see Kowal et al. 2003). The thermal gas component is currently treated as an adiabatic medium.

The transport of the CR component is described by the diffusion-advection equation

$$\frac{\partial e_{\rm cr}}{\partial t} + \boldsymbol{\nabla} \left(e_{\rm cr} \boldsymbol{V} \right) = \boldsymbol{\nabla} \left(\hat{K} \boldsymbol{\nabla} e_{cr} \right) - p_{\rm cr} \left(\boldsymbol{\nabla} \cdot \boldsymbol{V} \right) + Q_{\rm SN}, \tag{6}$$

where $Q_{\rm SN}$ represents the source term for the CR energy density: the rate of production of CRs injected locally in SN remnants and

$$p_{\rm cr} = (\gamma_{\rm cr} - 1) e_{\rm cr}, \quad \gamma_{\rm cr} = 14/9. \tag{7}$$

The adiabatic index of the CR gas $\gamma_{\rm cr}$ and the formula for diffusion tensor

$$K_{ij} = K_\perp \delta_{ij} + (K_\parallel - K_\perp) n_i n_j, \quad n_i = B_i / B, \tag{8}$$

are adopted following the argumentation by Ryu et al. (2003).

4. Numerical simulations

We performed numerical simulations in a 3D Cartesian domain 500pc $\times$ 1000pc $\times$ 1200pc , extending symmetrically around the galactic midplane from $z = -600$pc up to $z = 600$pc , with the resolution of $50 \times 100 \times 120$ grid zones in directions x, y and z, corresponding locally to cylindrical coordinates r, ϕ and z, respectively. The applied boundary conditions are periodic in the y-direction, sheared-periodic in the x direction and outflow in the z direction. The computational volume represents a 3D region of disk of a galaxy similar to the Milky Way.

The assumed disk rotation is represented locally by the angular velocity $\Omega = 0.05{\rm Myr}^{-1}$ and by a flat rotation curve corresponding to $q = 1$. We apply the vertical gravity profile determined for the Solar neighborhood (see Ferriere 1998 for the formula). We assume that supernovae explode with the frequency $2{\rm kpc}^{-2}{\rm Myr}^{-1}$, and assume that 10 % of the 10^{51}erg kinetic energy output from SN is converted into the CR energy. The CR energy is injected instantaneously into the ISM with a Gaussian radial profile ($r_{SN} = 50$pc) around the explosion center. The explosion centers are located randomly with a uniform distribution in the x and y directions and with a Gaussian distribution (scaleheight $H = 100$pc) in the vertical direction. The applied value of the CR parallel diffusion coefficient is $K_\parallel = 10^4 {\rm pc}^2 {\rm Myr}^{-1} = 3 \times 10^{27} {\rm cm}^2 {\rm s}^{-1}$ (i.e. 10 % of the realistic value) and

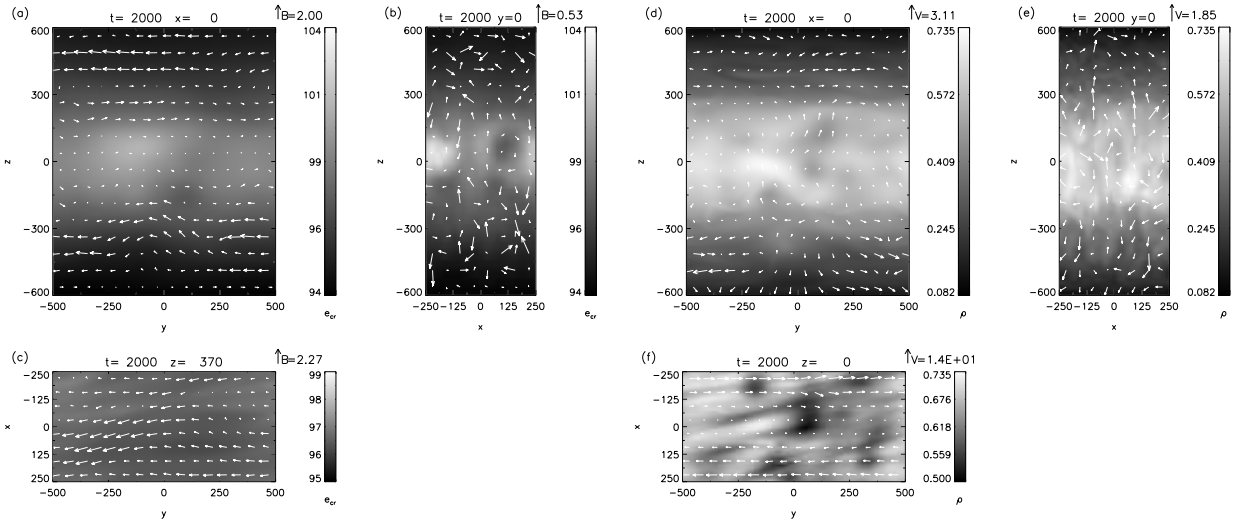

Fig. 1.— Slices through the computational volume at $t = 2000$Myr . Panels (a),(b) and (c) show CR energy density with vectors of magnetic field in yz, xz and xy planes respectively, panels (d), (e) and (f) show gas density with velocity vectors in the same planes.

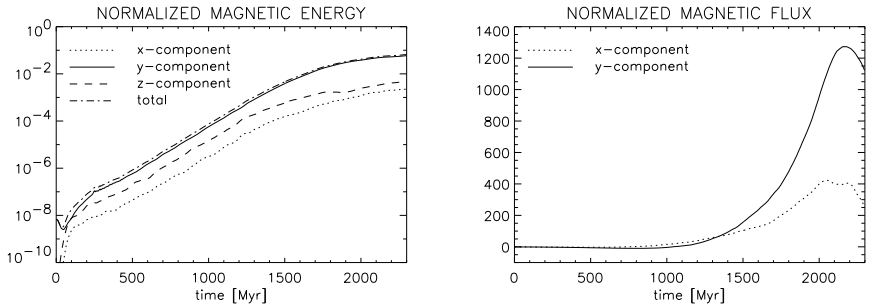

Fig. 2.— Evolution of magnetic field in the computational volume. The left panel shows the total magnetic energy normalized to the initial gas thermal energy (dash-dot line) along with normalized energies of azimuthal magnetic field (full line), radial magnetic field (dotted line) and vertical magnetic field (dashed line). The right panel shows the evolution of azimuthal magnetic flux $\times(-1)$ (full line) and radial magnetic flux $\times 10$ (dotted line), both normalized to the initial value of the azimuthal magnetic flux.

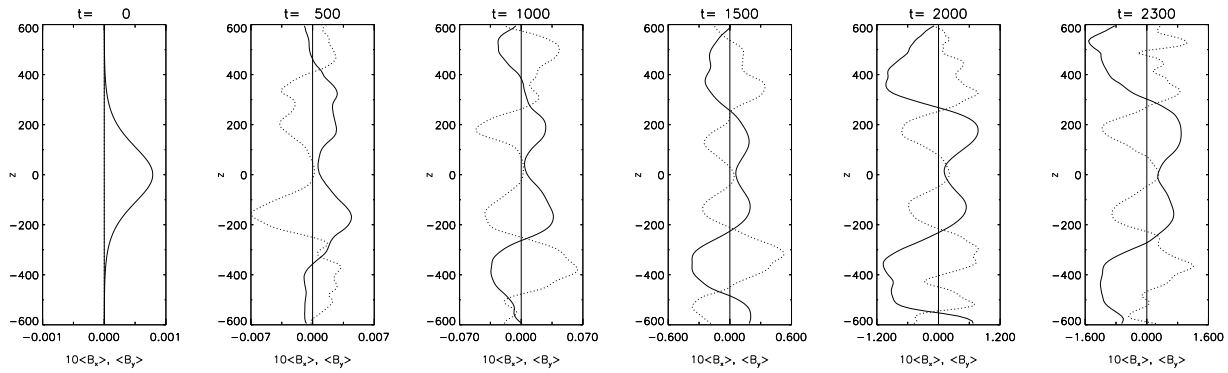

Fig. 3.— Vertical structure of the mean magnetic field for a sequence of time instants. Spatial averaging is done over planes z=const. Full line represents the mean azimuthal magnetic field and dotted line the radial magnetic field multiplied by 10. The amplification effect is reflected in the varying range of the horizontal axis.

the perpendicular one is $K_\perp = 10^3 \mathrm{pc}\ ^2\mathrm{Myr}^{-1} = 3 \times 10^{26} \mathrm{cm}^2\mathrm{s}^{-1}$.

The initial state of the system is a magnetohydrostatic equilibrium with a horizontal purely azimuthal magnetic field of the strength corresponding to $p_{\mathrm{mag}}/p_{\mathrm{gas}} = 10^{-8}$. The initial CR pressure in the initial state is equal to zero. The initial gas density at the galactic midplane is 3 H atoms cm^{-3} and the initial isothermal sound speed is $c_{\mathrm{si}} = 7\mathrm{km\ s}^{-1}$.

5. Structure of interstellar medium resulting from the CR-MHD simulations

In Fig. 1 we show the distribution of CR gas together with magnetic field, and thermal gas density together with and gas velocity in the computational volume at $t = 2000$ Myr.

One can notice in panel (a) a dominating horizontal alignment of magnetic vectors. The CR energy density is well smoothed by the diffusive transport in the computational volume. The vertical gradient of the CR energy density is maintained by the supply of CRs around the equatorial plane in the disk in the presence of vertical gravity. In panel (c) one can notice that at the height $z = 370$pc the dominating magnetic vectors are inclined with respect to the azimuthal direction, i.e. the radial magnetic field component is on average about 10 % of the azimuthal one.

The CR energy density is displayed in units in which the thermal gas energy density corresponding to $\rho = 1$ and the sound speed $c_{\mathrm{si}} = 7\mathrm{km\ s}^{-1}$ is equal to 1. We note that the CR energy density does not drop to zero at the lower and upper z boundaries due to our choice of outflow boundary conditions for the CR component. We note also that almost constant mean vertical gradient of CR energy density is maintained during the whole simulation.

The velocity field together with the distribution of gas density, is shown in the next panels (d), (e) and (f). The shearing pattern of velocity can be noticed in the horizontal slice (f). The vertical slices (d) and (e) show the stratification of gas by the vertical gravity, acting against the vertical gradients of thermal, CR and magnetic pressures.

6. Amplification and structure of the mean magnetic field

In the following Fig. 2 we show how efficient is the amplification of mean magnetic field resulting from the continuous supply of CRs in supernova remnants. First we note the growth of the total magnetic energy, by 7 orders of magnitudes during the period of 2 Gyr. Starting from $t \sim 300$ Myr the growth of magnetic energy represents a straight line on a logarithmic plot, which means that the magnetic energy grows exponentially. The e-folding time of magnetic energy determined for the period $t = 400 \div 1500$ Myr is 115 Myr. Around $t = 1500$ Myr, the growth starts to slow down as the magnetic energy approaches an

equipartition with the gas energy.

The other three curves in the left panel of Fig. 2 show the growth of energy of each magnetic field component. It is apparent that the energy of radial magnetic field component is almost an order of magnitude smaller than the energy of vertical magnetic field component which is almost one order of magnitude smaller than the energy of the azimuthal one. This indicates that the dynamics of the system is dominated by the buoyancy of CRs and that magnetic reconnection efficiently cancels the excess of the random magnetic fields.

In the right panel of Fig. 2 we show the time evolution of the normalized, mean magnetic fluxes $\Phi_x(t)/\Phi_y(t=0)$ and $\Phi_y(t)/\Phi_y(t=0)$, where $\Phi_x(t)$ and $\Phi_y(t)$ are respectively magnetic fluxes at moment t, threading vertical planes perpendicular to x and y axes respectively, and averaging is done over all possible planes of a given type. We find that the radial magnetic flux Φ_x starts to deviate from zero, as a result of Coriolis force and open boundary conditions. Due to the presence of differential rotation the azimuthal magnetic field is generated from the radial one. The azimuthal flux grows up by a factor of 10 in the first 800 Myr of the system evolution and then drops suddenly, reverts and continues to grow with the opposite sign undergoing amplification by more three orders of magnitudes, with respect to the initial value.

In order to examine the structure of the mean magnetic field we average of B_x and and B_y across constant z-planes. The results are presented in Fig. 3 for $t = 0$ (the initial magnetic field) and then for $t = 500$, 1000, 1500, 2000 and 2300 Myr. We find that the mean magnetic field grows by a factor of 10 within about 500 Myr, which gives an e-folding time close to 250 Myr. We note that an apparent wavelike vertical structures in $\langle B_x \rangle$ and $\langle B_y \rangle$ formed from the initial purely azimuthal, unidirectional state of B_y and $B_x = 0$. The evolved mean magnetic field configuration reaches a quasisteady pattern which is growing in magnitude with apparent vertical reversals of both components of the mean magnetic field. We note also that the magnetic field at the disk midplane remains relatively weak.

A striking property of the mean magnetic field configuration is the almost ideal coincidence of peaks of the oppositely directed radial and azimuthal field components. This feature corresponds to a picture of an $\alpha - \Omega$-dynamo: the azimuthal mean magnetic component is generated from the radial one and vice versa.

In order to understand better what kind of dynamo operates in our model, we computed the y-component of the electromotive force $\langle \mathcal{E}_{\mathrm{mf},y} \rangle = \langle v_z B_x - v_x B_z \rangle$, averaged over constant z-planes and checked that $\partial \langle B_x \rangle / \partial t \simeq -\partial \langle \mathcal{E}_{\mathrm{mf},y} \rangle / \partial x$ with a reasonable accuracy. However, we found that the space averaged $\mathcal{E}_{\mathrm{mf},y}$ fluctuates rapidly in time, so that the approximation of $\langle \mathcal{E}_{\mathrm{mf},y} \rangle$ by $\alpha_{yy} \langle B_y \rangle$, (where α_{yy} is a component of the fluid helicity tensor), implies that α_{yy} oscillates rapidly in time. This property points our model toward the incoherent $\alpha - \Omega$ dynamo described by Vishniac & Brandenburg (1997). Finally, we checked that the magneto-rotational instability (Balbus and Hawley 1991) does not seem to play a significant role in our dynamo model. Due to the weakness of the initial magnetic field, the wavelength of most unstable mode of this instability remains shorter than the cell size for the first half of the simulation time.

7. Conclusions

We have described the first numerical experiment in which the effect of amplification of the large scale galactic magnetic field was achieved by the (1) continuous (although intermittent in space and time) supply of CRs into the interstellar medium, (2) shearing motions due to differential rotation and (3) the presence of an explicit resistivity of the medium.

We observed in our experiment the growth of magnetic energy by seven orders of magnitude and the growth of magnetic flux by a factor of 1300 in 2150 Myr of the system evolution. We found that the large scale magnetic field grows on a timescale 250 Myr, which is close to the period of galactic rotation.

Therefore the galactic dynamo driven by CRs appears to work very efficiently, as it was suggested by Parker (1992). It is a matter of future work to verify whether the presented model is a fast dynamo, i.e. whether it works with a similar efficiency in the limit of vanishing resistivity.

This work was supported by the Polish Committee for Scientific Research (KBN) through the

grants PB 404/P03/2001/20 and PB 0249/P03/2001/21. We thank Mordecai Marc Mac Low for the preliminary version of shearing boundary conditions. The presented computations have been performed on the HYDRA computer cluster in Toruń Centre for Astronomy.

REFERENCES

Balbus, S.A., Hawley, J.F. 1991, ApJ, 376, 214

Ferriere, K. 1998, ApJ, 497, 759

Hanasz, M., Lesch, H. 1998, A&A, 332, 77

Hanasz, M. Lesch, H. 2000, ApJ, 543, 235

Hanasz, M., Otmianowska-Mazur, K., Lesch, H. 2002, A&A, 386, 347

Hanasz, M., Lesch, H. 2003a, A&A, 404, 389

Hanasz, M., Lesch, H. 2003b, A&A, 412, 331

Hawley, J.F., Gammie, C.F., Balbus, S.A. 1995, ApJ, 440, 442

Jokipii, J.R.: 1999, *in* J. Franco and A. Carraminana (eds.) *Interstellar Turbulence*, Cambridge University Press, 70-78.

Kowal, G., Hanasz, M., Otmianowska-Mazur, K., 2003, A&A, 404, 533

Lesch, H., Hanasz, M. 2003, A&A, 401, 809

Parker, E.N. 1992, ApJ, 401, 137

Ryu, D., Kim, J., Hong, S.S., Jones, T.W. 2003, Apj, 589, 338

Stone, J.M., Norman, M.L, 1992a, ApJS, 80, 753

Stone, J.M., Norman, M.L, 1992b, ApJS, 80, 791

Vishniac, E.T., Brandenburg, A. 1997, ApJ, 475, 263

This 2-column preprint was prepared with the AAS LaTeX macros v5.2.